Conformational States in Denaturants of Cytochrome c and Horseradish Peroxidases Examined by Fluorescence and Circular Dichroism †

ARTICLE *in* BIOCHEMISTRY · MARCH 1998

Impact Factor: 3.02 · DOI: 10.1021/bi971032a · Source: PubMed

3 AUTHORS, INCLUDING:

George Tsaprailis
The University of Arizona
43 PUBLICATIONS **2,685** CITATIONS

SEE PROFILE

Conformational States in Denaturants of Cytochrome *c* and Horseradish Peroxidases Examined by Fluorescence and Circular Dichroism[†]

George Tsaprailis, Doreen Wing Sze Chan, and Ann M. English*

Department of Chemistry and Biochemistry, Concordia University, 1455 de Maisonneuve Boulevard West, Montreal, Quebec, Canada H3G 1M8

Received May 2, 1997; Revised Manuscript Received October 15, 1997[⊗]

ABSTRACT: Steady-state fluorescence and circular dichroism (CD) were used to examine the unfolding in denaturants of recombinant cytochrome *c* peroxidase [CCP(MI)] and horseradish peroxidase (HRP) in their ferric forms. CCP(MI) unfolds in urea and in guanidine hydrochloride (GdHCl) at pH 7.0, while HRP loses its secondary structure only in the presence of GdHCl. CCP(MI) unfolds in urea by two distinct steps as monitored by fluorescence, but the loss of its secondary structure as monitored by UV/CD occurs in a single step between 3.4 and 5 M urea and 1.5 and 2.5 M GdHCl. The localized changes detected by fluorescence involve the CCP(MI) heme cavity since the Soret maximum red-shifts from 408 to 416 nm, and the heme CD changes examined in urea are biphasic. The polypeptide of HRP also loses secondary structure in a single step between 1.2 and 2.7 M GdHCl as monitored by UV/CD, and a fluorescence-monitored transition involving conformational change in the Trp117-containing loop occurs above 4 M GdHCl. Free energies of denaturation extrapolated to 0 M denaturant ($\Delta G_{d,aq}$) of ∼6 and ∼4 kcal/mol were calculated for CCP(MI) and HRP, respectively, from the UV/CD data. The refolding mechanisms of the two peroxidases differ since heme capture in CCP(MI) is synchronous with refolding while apoHRP captures heme *after* refolding. Thus, the denatured form of apoHRP does not recognize heme and has to correctly refold *prior* to heme capture. The half-life for unfolding of native HRP in 6 M GdHCl is slow (519 s) compared to that for CCP(MI) (14.3 s), indicating that HRP is kinetically much more stable than CCP(MI). Treatment with EDTA and DTT greatly destabilizes HRP, and unfolding in 4 M GdHCl occurs with $t_{1/2} = 0.42$ s.

Heme peroxidases oxidize a wide variety of organic and inorganic substrates by H_2O_2 according to the following equation:

$$H_2O_2 + 2AH \rightarrow 2H_2O + 2A \quad (1)$$

The last decade has seen an explosion in the X-ray structure determination of heme proteins and heme peroxidases in particular. Notable among these are the structures of cytochrome *c* peroxidase (CCP)[1] (Finzel et al., 1984), lignin peroxidase (LIP) (Poulos et al., 1993), *Arthromyces ramosus* peroxidase (ARP) (Kunishima et al., 1994), *Coprinus cinereus* peroxidase (CIP) (Petersen et al., 1994), pea ascorbate peroxidase (APX) (Patterson & Poulos, 1995), manganese peroxidase (MnP) (Sundaramoorthy et al., 1994), and peanut peroxidase (PNP) (Schuller et al., 1996). An inspection of the three-dimensional structures of these peroxidases reveals that they possess similar secondary structure (Poulos & Fenna, 1994; English & Tsaprailis, 1995). Moreover, they have been grouped into the plant peroxidase superfamily which consists of evolutionary-related heme peroxidases from bacteria, fungi, and plants (Welinder, 1992). Structural elements are also conserved around the prosthetic group in heme peroxidases (Garavito et al., 1994), emphasizing their evolutionary relationship.

Horseradish peroxidase isoenzyme C (HRP) is the most studied heme peroxidase (Dunford, 1991). Despite this, the X-ray structure has just been solved for this isoenzyme (T. L. Poulos, personal communication). The secondary and tertiary structures of HRP are very similar to those of ARP, CIP, LIP, and PNP since they all share a number of common structural features. These include Ca^{2+} binding sites proximal and distal to the heme, four disulfide bridges, and a number of N-glycosylation sites (Welinder, 1992; Poulos, 1993; Poulos & Fenna, 1994; English & Tsaprailis, 1995). The newly-solved X-ray structure of HRP shows that its secondary structure is essentially identical to that of PNP with which it shares 50% sequence homology. Moreover, the four disulfide bridges, the Ca^{2+} binding sites, and other key residues in the proximal and distal sides of the heme

[†] This research was funded by a grant from the Natural Sciences and Engineering Research Council of Canada (NSERC) to A.M.E.

* Author to whom correspondence should be addressed. Telephone: 514-848-3338. Fax: 514-848-2868. E-mail: english@vax2.concordia.ca.

[⊗] Abstract published in *Advance ACS Abstracts,* December 15, 1997.

[1] Abbreviations: APX, pea cytosolic ascorbate peroxidase; ARP, *Arthromyces ramosus* peroxidase; CCP, yeast cytochrome *c* peroxidase; CCP(MI), recombinant cytochrome *c* peroxidase from *Escherichia coli*; CD, circular dichroism; CIP, *Coprinus cinereus* peroxidase; DTT, dithiothreitol; EDTA, ethylenediaminetetraacetic acid; GdHCl, guanidine hydrochloride; HRP, horseradish peroxidase isoenzyme C; LIP, lignin peroxidase; Mb, myoglobin; MnP, manganese peroxidase; NATA, *N*-acetyltryptophanamide; NAYA, *N*-acetyltyrosinamide; NMR, nuclear magnetic resonance; Phe, phenylalanine; PNP, peanut peroxidase; RNase T_1, ribonuclease T_1; Trp, tryptophan; Tyr, tyrosine.

S0006-2960(97)01032-5 CCC: $15.00
Published on Web 01/30/1998

are conserved between HRP and PNP, although they differ slightly around the entrance to the heme cavity (T. L. Poulos, personal communication).

The first crystal structure obtained for a heme peroxidase was that of CCP published in 1980 (Poulos et al., 1980), and a 1.7 Å resolution structure appeared in 1984 (Finzel et al., 1984). The structure can be divided into N- and C-terminal domains, and the heme is in a cavity at the domain interface. The secondary structure is dominated by α-helices with only a small amount of β-sheet in the proximal domain. CCP has served in large part as the archetypical heme peroxidase, but despite the similarity of its tertiary and secondary structures to those of other enzymes in the plant peroxidase superfamily, CCP does not possess disulfide bridges, bound Ca^{2+}, nor glycosylation sites (Bosshard et al., 1991). A need for an examination of the effects of these structural elements on the conformational stabilities of related heme peroxidases was noted by Holzbaur et al. (1996). Heme capture on folding of peroxidases is also anticipated to depend on the presence of stabilizing structural elements since, for example, recombinant HRP has been isolated in inclusion bodies largely as the apoprotein and peroxidase activity could be restored only on refolding the protein in the presence of added Ca^{2+} as well as heme (Smith et al., 1990).

A comparative study of the conformational stability of CCP and HRP in denaturants was undertaken to probe the effects of the additional stabilizing elements in HRP. Specifically, conformational changes in recombinant cytochrome *c* peroxidase from *Escherichia coli* [CCP(MI)] and HRP were monitored by steady-state protein fluorescence and circular dichroism. Unfolding intermediates were observed for the peroxidases in urea and guanidine hydrochloride (GdHCl) at pH 7.0 by fluorescence, but the properties of the intermediates are very different for the two peroxidases as shown by Soret and heme CD absorption measurements. Heme capture by CCP(MI) and HRP on refolding of the denatured peroxidases was also investigated by steady-state fluorescence, Soret absorption, and CD.

EXPERIMENTAL PROCEDURES

Materials

Grade I, salt-free, lyophilized horseradish peroxidase isoenzyme C (HRP) (EC 1.11.1.7) was obtained from Boehringer Mannheim and used without further purification. Recombinant cytochrome *c* peroxidase from *E. coli* [CCP(MI)] (EC 1.11.1.5) was isolated following a previously described procedure (Fishel et al., 1987). Ultrapure-grade urea was purchased from Anachemia, and guanidine hydrochloride (GdHCl) (>99%) was obtained from Sigma. *N*-Acetyltryptophanamide (NATA) and *N*-acetyltyrosinamide (NAYA) standards were also purchased from Sigma, and DTT and EDTA were obtained from ICN. All solutions were prepared using distilled water (specific resistance of 18 MΩ) from a Barnstead Nanopure system. Absorption spectra were recorded on a Hewlett-Packard 8451A diode array spectrophotomer, fluorescence spectra on a Shimadzu Model RF-5000 spectrofluorophotometer, and CD spectra on a JASCO J-710 spectropolarimeter purged with N_2 at a flow rate of 5 L/min.

Methods

Denaturation of CCP(MI) and HRP as Monitored by Steady-State Fluorescence. Stock protein solutions were prepared in 100 mM sodium phosphate buffer (pH 7.0) using $\epsilon_{408} = 102\ mM^{-1}\ cm^{-1}$ (Fishel et al., 1987) and $\epsilon_{403} = 102\ mM^{-1}\ cm^{-1}$ (Veitch & Williams, 1990) for CCP(MI) and HRP, respectively. The concentrations of NATA ($\epsilon_{280} = 5.69\ mM^{-1}\ cm^{-1}$) and NAYA ($\epsilon_{276} = 1.49\ mM^{-1}\ cm^{-1}$) were also determined spectrophotometrically (Edelhoch, 1967). GdHCl (0−6.4 M) and urea (0−8 M) solutions of known concentration were prepared by weight in 100 mM sodium phosphate buffer (pH 7.0). The proteins were allowed to denature for 20−24 h at ambient temperature prior to recording the fluorescence spectra, and the concentrations used in the fluorescence measurements were 1 μM CCP(MI) and 2 μM HRP. The emission of the blank (denaturant in buffer) was subtracted from that of the protein samples prior to integration. The steady-state fluorescence intensities of CCP(MI) were standardized to 7 μM NATA and those of HRP to a solution containing 2 μM NATA and 10 μM NAYA since the fluorescence intensity ($\lambda_{ex} = 280$ nm) of fully denatured 1 μM CCP(MI) is equal to that of 7 μM free Trp (Fox et al., 1994) while that of 2 μM HRP is equal to 2 μM Trp and 10 μM Tyr (Pappa & Cass, 1993; Das & Mazumdar, 1995). The integrated intensity obtained for the standards under identical conditions was taken to be 100%.

To test the reversibility of denaturation, ~30 μM solutions of CCP(MI) and HRP were incubated for 20−24 h in 8 M urea (pH 7.0) and 6 M GdHCl (pH 7.0), respectively. Following incubation, the samples were diluted to give the desired final concentrations of denaturant and then incubated for another 20−24 h before the fluorescence spectra were recorded as described above.

Denaturation of CCP(MI) and HRP as Monitored by CD Spectroscopy. Stock protein solutions (~30 μM) prepared in 100 mM sodium phosphate buffer (pH 7.0) were diluted to ~5 μM for backbone CD-monitored denaturation measurements. Backbone refolding of HRP and CCP(MI) was examined following denaturation for 20−24 h of ~100 μM stock HRP and ~80 μM CCP(MI) in 6 M GdHCl (pH 7.0) and 8 M urea (pH 7.0), respectively. All CD spectra in the backbone region (210−240 nm; UV/CD) were recorded in a 0.05-cm path-length cell (~150 μL) using a scan speed of 100 nm/min with a response time of 0.25 s. The UV/CD spectra reported here are the average of five scans at 0.2-nm resolution and a bandwidth of 1 nm. The observed ellipticity θ (millidegrees) was divided by ($10 \times C \times l$) to convert to molar ellipticity [θ], where C is the concentration (moles per liter) and l the path-length (centimeters) (Sievers, 1978). For the CD spectra in the aromatic and Soret regions (240−480 nm), a 0.5-cm path-length cell was used at a protein concentration of ~10 μM. All other parameters were the same as those used in the UV/CD measurements.

Analysis of the UV/CD Transition Curves. As discussed below, the unfolding of the CCP(MI) and HRP backbones as monitored by UV/CD appears to follow a two-state transition and hence was analyzed according to the method of Pace et al. (1990):

$$N \rightleftharpoons U \qquad (2)$$

where N is the native protein and U is the unfolded protein.

The equilibrium constant between the unfolded and native states is given by

$$K = [\mathrm{U}]/[\mathrm{N}] \tag{3}$$

K is related to the fraction of unfolded protein (F_U), and the standard Gibbs free energy of denaturation (ΔG_d) by

$$\Delta G_d = -RT \ln K = -RT \ln(F_U/1 - F_U) \tag{4}$$

where R is the universal gas constant and T is the absolute temperature. F_U and hence K may be calculated by recording the change in molar ellipticity $[\theta]$ as follows:

$$F_U = ([\theta]_N - [\theta]_{obs})/([\theta]_N - [\theta]_U) \tag{5a}$$

$$K = ([\theta]_N - [\theta]_{obs})/([\theta]_{obs} - [\theta]_U) \tag{5b}$$

where $[\theta]_{obs}$ is the observed molar ellipticity, and $[\theta]_N$ and $[\theta]_U$ are the values of $[\theta]$ characteristic of the native and unfolded conformations, respectively. ΔG_d and K depend on the denaturant concentration according to the linear extrapolation method (Pace, 1986):

$$\Delta G_d = \Delta G_{d,aq} - m[\text{denaturant}] \tag{6}$$

where $\Delta G_{d,aq}$ is the value of ΔG_d at zero concentration of denaturant and m is a measure of the dependence of ΔG_d on denaturant concentration. $\Delta G_{d,aq}$ represents the free energy under normal conditions (aqueous solutions in the absence of denaturant at room temperature) and hence defines the conformational stability of a protein that undergoes a single N ⇌ U transition (Pace, 1990).

Steady-State Fluorescence-Monitored Denaturation of EDTA- and DTT-Treated HRP. Solutions of 10 μM HRP were incubated with (1) 3 mM DTT, (2) 30 mM DTT, (3) 2 mM EDTA, and (4) 3 mM DTT + 2 mM EDTA for 18 h at 4 °C before aliquots of the protein were unfolded in 0−6 M GdHCl (pH 7.0) for 20−24 h at ambient temperature. The integrated fluorescence intensities (300−450 nm) were normalized relative to 2 μM NATA/10 μM NAYA solutions that had been similarly treated with DTT and EDTA.

Kinetics of Unfolding of CCP(MI) and HRP in Denaturants. The time-dependent unfolding of both peroxidases was investigated at pH 7.0 by diluting 5 μM CCP(MI) into 8 M urea and 10 μM HRP into 6 M GdHCl. Following rapid manual mixing, quartz cuvettes containing 1 μM CCP(MI) or 2 μM HRP in denaturant were quickly placed in the spectrofluorophotometer, and the fluorescence intensity at 350 nm was monitored as a function of time. The excitation wavelength was 280 nm, and the emission and excitation slits were 5 nm. The time-dependent fluorescence increase was fitted by a single exponential. The time courses of unfolding of EDTA- and DTT-treated HRP were also examined. The kinetics of HRP unfolding following incubation with *both* EDTA and DTT were investigated by stopped-flow in 4 M GdHCl. Equal volumes of 8 M GdHCl and 10 μM HRP in 3 mM DTT/2 mM EDTA were mixed, and the fluorescence was measured using an Applied Photophysics SX17MV stopped-flow spectrofluorophotometer. The growth of the fluorescence intensity at 350 nm (λ_{ex} = 280 nm; 5 nm excitation and emission slits) was also fitted by a single exponential.

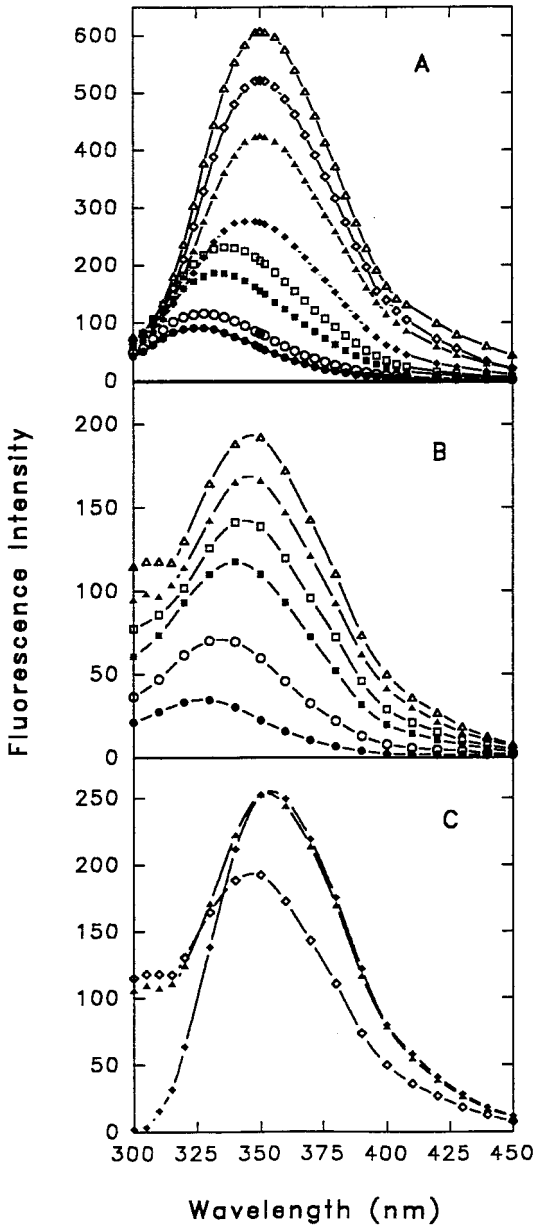

FIGURE 1: Fluorescence spectra at pH 7.0 of (A) 1 μM CCP(MI) in 0 M (●), 1 M (○), 3 M (■), 4 M (□), 5 M (◆), 5.5 M (▲), 6 M (◇), and 8 M (△) urea; (B) 2 μM HRP in 0 M (●),1 M (○), 1.6 M (■), 2 M (□), 4.4 M (▲), and 6 M (△) GdHCl; (C) 2 μM HRP (◇), 2 μM L-NATA/10 μM L-NAYA (▲), and 2 μM L-NATA (◆) in 6.4 M GdHCl. Excitation 280 nm; slits 5 nm; scan rate 102 nm/min.

RESULTS

Denaturation of CCP(MI) and HRP as Monitored by Steady-State Fluorescence. Quenching of peroxidase fluorescence emission is caused by the presence of the heme prosthetic group (Willis et al., 1990). Relief of heme quenching, as well as a red-shift in the steady-state fluorescence of CCP(MI), is observed when the protein is incubated in increasing concentrations of urea at pH 7.0. Both of these observations are indicative of protein unfolding and Trp exposure to the aqueous environment (Burnstein et al., 1973). The fluorescence intensities of CCP(MI) in varying concen-

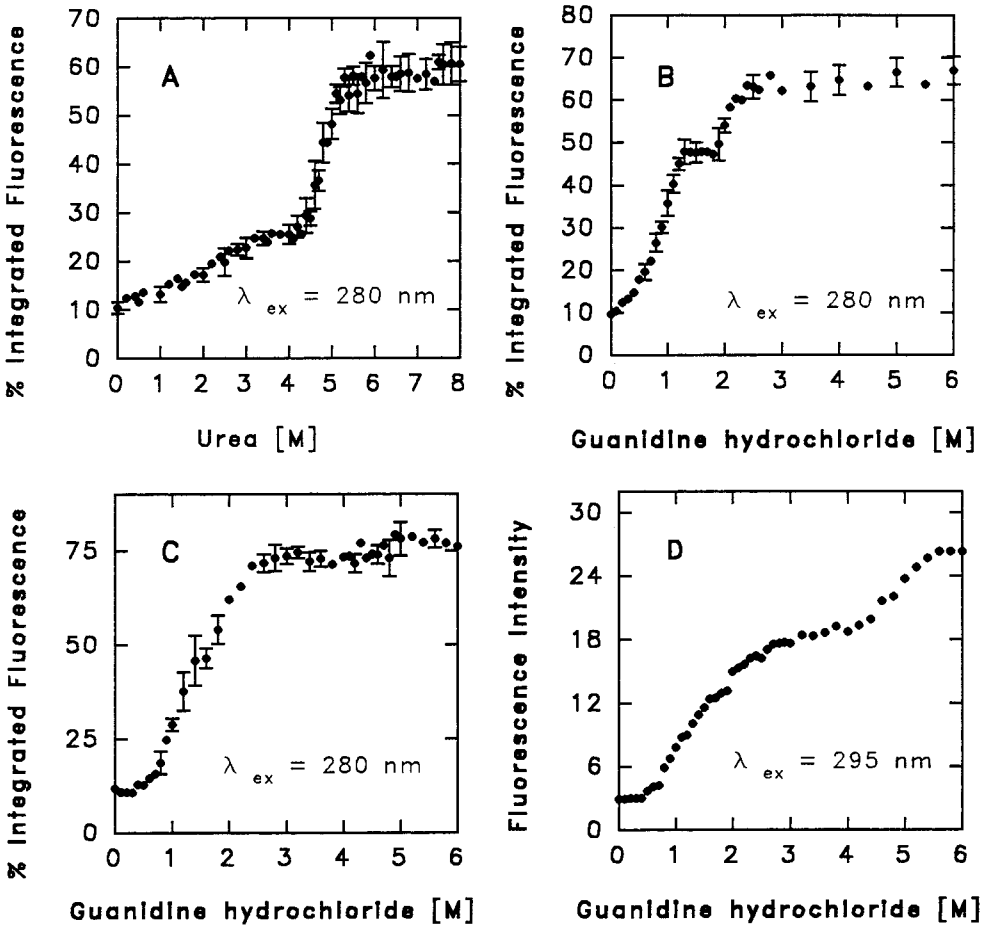

FIGURE 2: Relative integrated fluorescence (300−450 nm) intensities at pH 7.0 of (A) 1 μM CCP(MI) vs urea concentration, (B) 1 μM CCP(MI) vs GdHCl concentration, (C) 2 μM HRP vs GdHCl concentration. The points represent the average of two to eight measurements for CCP(MI) and two or three measurements for HRP. The intensities are plotted relative to 7 μM NATA for CCP(MI) and 2 μM NATA/10 μM NAYA for HRP under the same conditions. Excitation 280 nm; slits 5 nm; scan rate 102 nm/min. (D) Fluorescence intensity at 350 nm of 2 μM HRP vs GdHCl concentration on excitation at 295 nm (note: since Trp is selectively excited at 295 nm, a plot of integrated intensity between 300 and 450 nm would have the same shape as that shown here for intensity at 350 nm). Slits 5 nm; scan rate 402 nm/min.

trations of urea at pH 7.0 are shown in Figure 1A. The emission maximum gradually shifts from 325 ± 2 nm in 0 M urea to 350 ± 2 nm in ≥5.5 M urea. The same fluorescence behavior is seen when CCP(MI) is incubated with increasing concentrations of GdHCl at pH 7.0 (data not shown), but since GdHCl is a stronger denaturant than urea (Rainer & Rainer, 1990), the emission maximum occurs at 350 nm in ≥2.2 M GdHCl. Relief of heme quenching is also observed when HRP is incubated with GdHCl at pH 7.0 (Figure 1B). A red-shift from the 326 ± 2 nm emission maximum in buffer occurs at ≥ 0.2 M GdHCl, and the maximum has fully red-shifted to 348 ± 2 nm in 2.6 M GdHCl. HRP denaturation in urea was not monitored since our observations and those of Pappa and Cass (1993) reveal that HRP retains significant secondary structure in the presence of 8 M urea as monitored by UV/CD.

Excitation wavelength-dependent fluorescence is observed for HRP but not for CCP(MI). Figure 1C, which shows the fluorescence intensity of HRP, a NATA/NAYA mixture, and NATA in 6.4 M GdHCl (pH 7.0), clearly indicates that Tyr residues contribute to the fluorescence profile of HRP on excitation at 280 nm. A distinct maximum due to Tyr fluorescence (Creighton, 1993) is observed at 303 nm in the HRP spectra, and this maximum disappears on 295-nm excitation (data not shown). The emission spectrum of CCP(MI) in both urea and GdHCl resembles that in Figure 1C of the Trp standard (NATA) on excitation at 280 or 295 nm.

Figure 2A summarizes the integrated fluorescence intensity of CCP(MI) relative to NATA as a function of urea concentration. It can be seen that CCP(MI) does not unfold in urea by a simple two-state process. Rather, a stable intermediate appears at 3−4 M urea, followed by a sharp rise in the relative fluorescence intensity above 4 M urea which levels off at ∼60 ± 4% at 8 M urea. A plot of the observed fluorescence intensity at 350 nm (data not shown) is coincident with the relative integrated intensity (300−450 nm) of CCP(MI) (Figure 2A), consistent with Trp emission dominating CCP(MI) fluorescence due to efficient Tyr → Trp energy transfer (Fox et al., 1994). A two-step unfolding process is also seen when CCP(MI) is incubated with GdHCl (Figure 2B). A stable intermediate appears at 1.3−1.8 M GdHCl which is converted to the denatured state (∼65% relative fluorescence) above 2.5 M GdHCl. Thus, the denaturation of CCP(MI) as monitored by steady-state fluorescence is best described by

$$N \rightleftharpoons I \rightleftharpoons U \qquad (7)$$

where I represents an intermediate state in the equilibrium

unfolding process. The relative fluorescence of the intermediate I is ~25% in urea and ~50% in GdHCl, revealing that the CCP(MI) intermediate has looser structure in GdHCl compared to urea, unlike the final denatured forms which possess similar relative fluorescence (60−65%) in both denaturants.

The fluorescence-monitored unfolding behavior of HRP in GdHCl is presented in Figure 2C. Two fluorescence-monitored transitions are also observed for HRP but at higher GdHCl concentrations than in CCP(MI). The increase in protein fluorescence observed above 4 M GdHCl is much less pronounced on excitation at 280 nm (Figure 2C) than at 295 nm, the wavelength which preferentially excites the single Trp117 in HRP (Das & Mazumdar, 1995) (Figure 2D). Hence, the second transition in HRP is associated with a relaxation of the Trp117-containing extended chain. Since the unfolding intermediate occurs *after* loss of secondary structure and heme (see discussion below), the fluorescence-monitored denaturation of HRP occurs by a different mechanism than that of CCP and is better described by

$$N \rightleftharpoons U' \rightleftharpoons U \qquad (8)$$

Renaturation of CCP(MI) and HRP as Monitored by Steady-State Fluorescence. CCP(MI) renaturation likely occurs by the same mechanism as denaturation since both curves are similar (Figure 3A,B). HRP denaturation and renaturation, on the other hand, must occur by different mechanisms since, as can be seen from Figure 3C, renaturation involves refolding of the polypeptide prior to heme capture below 1 M GdHCl. Both renatured peroxidases exhibit higher fluorescence intensities due to incomplete heme capture during renaturation, but addition of exogenous heme quenched the fluorescence to the levels seen before denaturation.

Heme Soret Absorption and CD of Denatured CCP(MI) and HRP. The Soret absorption of the peroxidases was recorded in various concentrations of denaturants following the fluorescence measurements. At low denaturant concentration (1 M urea, 0.3 M GdHCl), the intensity of the Soret band of CCP(MI) at 408 nm is diminished (Figure 4A,B). A sharpening and red-shifting of the Soret to 416 nm is observed in 3.8 M urea and 1.3 M GdHCl, denaturant concentrations corresponding to those at which the unfolding intermediates of CCP(MI) have reached their maximum concentrations (Figure 2A,B). The GdHCl intermediate has a less intense 416-nm band, which together with its high fluorescence (~50%), indicates that it must have lower affinity for heme than the urea intermediate with only ~25% fluorescence. At denaturant concentrations above the transition regions, the Soret bands broaden again and blue-shift, and the resultant spectra in 8 M urea and 6 M GdHCl are nearly identical to those of free hemin under the same conditions (Figure 4C). The heme CD absorption of CCP(MI) at 410 nm as a function of urea is plotted in Figure 4D. The stable intermediate seen in the fluorescence-monitored unfolding of CCP(MI) and in the Soret spectra is also clearly observed in heme-CD-monitored denaturation which is a more sensitive probe of the CCP(MI) N ⇌ I transition than fluorescence.

The Soret absorption of HRP at different concentrations of GdHCl is shown in Figure 5A. No red-shift is observed

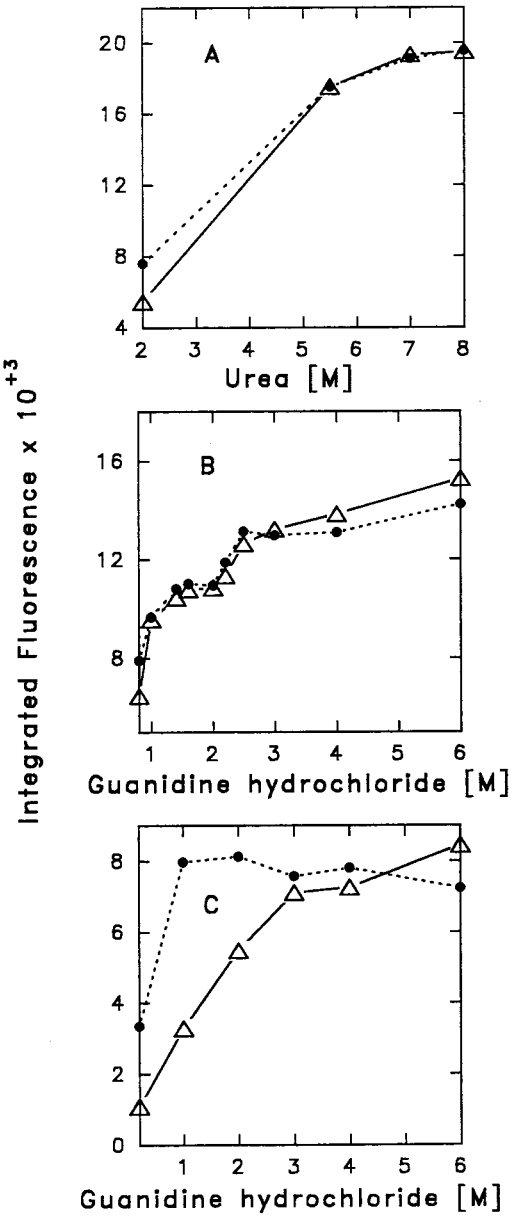

FIGURE 3: Integrated fluorescence intensity (300−450 nm) at pH 7.0 of (A) 1 μM CCP(MI) during unfolding (△) and refolding (●) in urea, (B) 1 μM CCP(MI) during unfolding (△) and refolding (●) in GdHCl, and (C) 1 μM HRP during unfolding (△) and refolding (●) in GdHCl. Excitation 280 nm; slits 5 nm; scan rate 102 nm/min.

in the Soret of HRP as the protein unfolds. Rather, a dramatic change is observed between 1 and 2 M GdHCl, and the Soret absorption in 3 M GdHCl resembles that of free hemin in 6 M GdHCl (Figure 4C). The smoothed heme CD spectra of HRP are shown in Figure 5B and reveal that in 2.6 M GdHCl the heme has dissociated from the polypeptide and lost the asymmetric character necessary for optical activity, consistent with the heme absorption data shown in Figure 5A.

The Soret absorption of CCP(MI) and HRP was also recorded during renaturation (spectra not shown). The Soret spectra of CCP(MI) undergoing renaturation were similar to those observed during denaturation (Figure 4A,B); specifically, the CCP(MI) intermediates at 416 nm were observed over the same denaturant concentrations on refolding. The Soret spectra of HRP showed that refolding of the polypep-

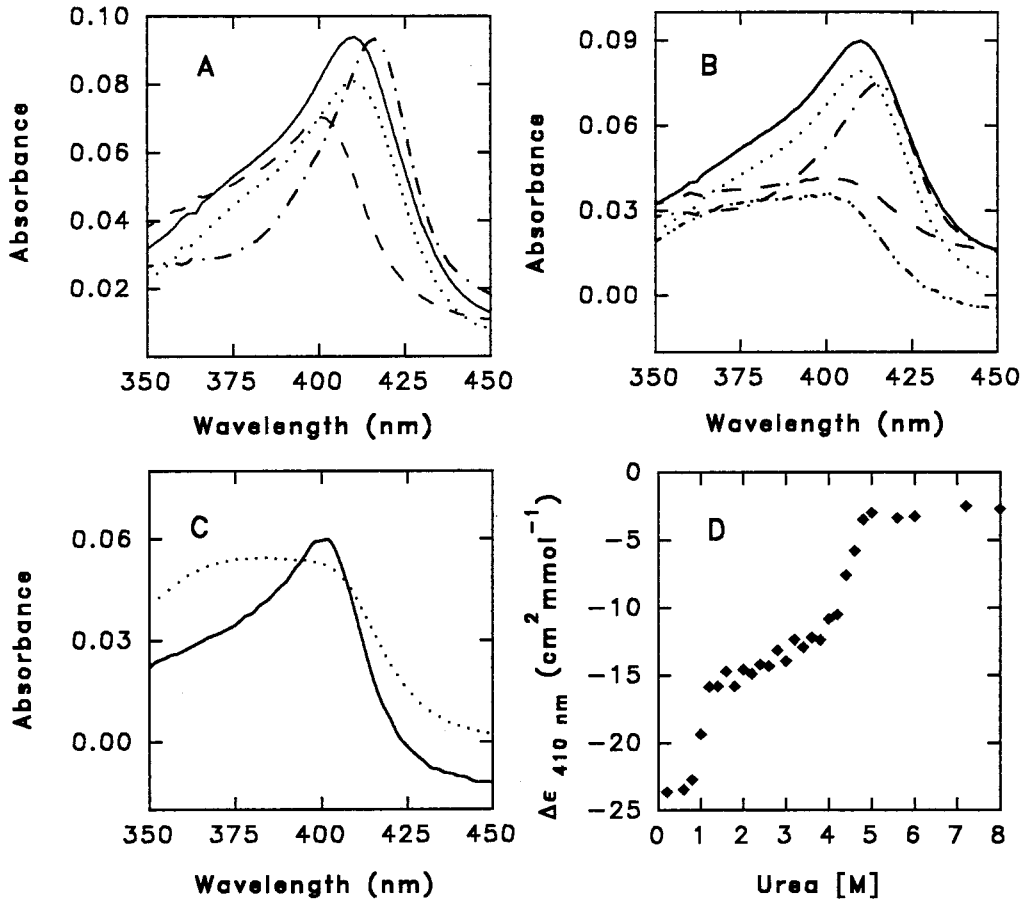

FIGURE 4: Soret absorption at pH 7.0 of (A) 1 μM CCP(MI) in 0 M (—), 1 M (···), 3.8 M (—·—), and 8 M (— —) urea; (B) 1 μM CCP(MI) in 0 M (—), 0.3 M (···), 1.3 M (—·—), 2 M (— —), and 6 M (—··—) GdHCl; (C) 0.44 μM hemin in 8 M (—) urea and 6 M (···) GdHCl. Path length 1 cm. (D) The molar CD absorption ($\Delta\epsilon$) at 410 nm of CCP(MI) vs urea at pH 7.0, where $\Delta\epsilon = [\theta]/3298$ (Kahn, 1979). The effective concentration of CCP(MI) in urea was 9.39 μM for the CCP(MI) heme CD measurements. Path length 0.5 cm.

tide was necessary for capture of the heme since no increase in Soret intensity was observed on renaturation until the GdHCl concentration was reduced to ≤1 M. Due to incomplete heme capture during refolding, the Soret intensity was only ~60% of that of the native protein in 0.2 M GdHCl. However, addition of excess hemin during renaturation resulted in 100% heme loading of HRP (data not shown).

Denaturation of CCP(MI) and HRP as Monitored by UV/CD. The loss in ellipticity of the backbone absorption at 222 nm of CCP(MI) and HRP vs urea or GdHCl concentration is shown in Figure 6. Unlike the fluorescence measurements (which are mainly sensitive to and report on localized changes with respect to the heme), the $[\theta]_{222}$ measurements indicate that the backbone of CCP(MI) unfolds in a single step with no accumulation of stable intermediates (Figure 6A,B). The backbone of HRP also unfolds in a single step (Figure 6C), and loss of secondary structure is almost complete before the fluorescence-detected intermediate (U′) appears above 2.5 M GdHCl (Figure 2C).

The refolding of the CCP(MI) and HRP backbones as monitored by $[\theta]_{222}$ is shown in Figure 7. The results indicate that the backbone unfolding and refolding pathways of CCP(MI) are essentially the same. However, there is a loss in backbone ellipticity as HRP refolds over 24 h. Allowing the protein to refold over a period of >24 h slightly increased the ellipticity of the *refolded* protein (data not shown), but on duplicate experiments it was observed that a fraction of HRP had precipitated and a decrease in heme absorbance was also observed in these samples. Precipitation of HRP in 6 M GdHCl is concentration dependent since it was observed at the high concentrations of stock HRP (~100 μM) required for the UV/CD refolding experiments, but not in the ~30 μM stock used in the fluorescence-monitored refolding experiments. A competition between folding and aggregation has also been reported for multidomain and multisubunit proteins on refolding. For example, the yield of refolded lactate dehydrogenase was protein concentration dependent with concentrations above ~0.1 μg/mL producing >25% aggregation (Garel, 1992).

From the above discussion, it can be concluded that denaturant-induced secondary structure loss in CCP(MI) and HRP is a reversible two-state process (eq 2). A nonlinear least-squares fit (Hughson & Baldwin, 1989; Betz & Pielak, 1992) to the UV/CD data in Figure 6 yielded the thermodynamic parameters $\Delta G_{d,aq}$ and m which are listed in Table 1.

Denaturation of EDTA- and DTT-Treated HRP as Monitored by Steady-State Fluorescence. The fluorescence intensity vs denaturant concentration of HRP following incubation with EDTA or DTT is shown in Figure 8. Incubation with 2 mM EDTA for 18 h makes HRP more sensitive to denaturation since the GdHCl concentration at half-maximum fluorescence ($[GdHCl]_{1/2}$) decreases from 2 to 0.45 M (Figure 2C vs 8A). Incubation of HRP with 3 and 30 mM DTT results in $[GdHCl]_{1/2}$ values of 1.3 and 0.9

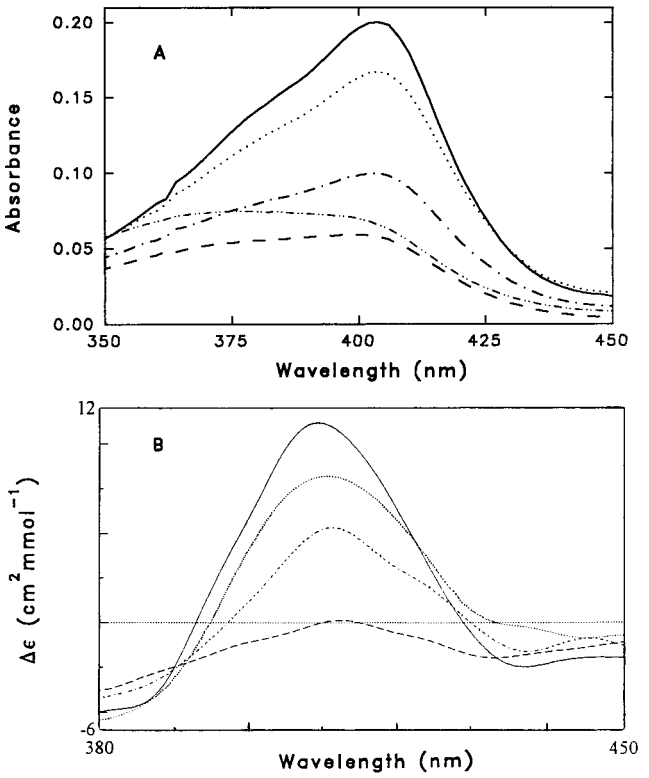

FIGURE 5: (A) Soret absorption of 2 μM HRP at pH 7.0 in 0 M (—), 1 M (···), 1.8 M (—·—), 2 M (— —), and 3 M (—··—) GdHCl. Path length 1 cm. (B) Smoothed CD spectra of 11 μM HRP in the aromatic and heme region (240−480 nm) at different GdHCl concentrations at pH 7.0: 0 M (—), 1 M (···), 1.8 M (—·—), and 2.6 M (— —). Path length 0.5 cm.

M, respectively (Figure 8B), indicating that the Ca^{2+} ions have a greater effect on the overall sensitivity of the protein to denaturant than the disulfide bridges. It should be noted that the number of free cysteines following an 18 h incubation with DTT were not determined because of the difficulty in carrying out such experiments in the presence of excess free thiol. However, since incubation of HRP with DTT results in decreased $[GdHCl]_{1/2}$ values, it can be assumed that reduction of one or more disulfides occurs in 3 mM DTT, and a higher number occur in 30 mM DTT. Consistent with this speculation, the relative integrated fluorescence (λ_{ex} = 280 nm) of HRP treated with 30 mM DTT is ∼20% higher than that of 3 mM DTT-treated HRP (Figure 8B), and the fluorescence maximum of the former has red-shifted from 326 to 342 nm in buffer only (data not shown). Figure 8C shows the fluorescence intensity at 350 nm in 0−6 M GdHCl following 295-nm excitation of untreated HRP and HRP incubated with 3 mM DTT. It is clearly evident from these denaturation curves that the sharp increase in fluorescence above 4 M GdHCl observed in untreated HRP is absent in DTT-treated HRP. This reveals that disulfide reduction affects the fluorescence behavior of Trp117 which is preferentially excited at 295 nm (Das & Mazumdar, 1995). It is of interest that after an 18 h incubation of HRP with *both* 2 mM EDTA and 3 mM DTT, Trp117 is largely solvent exposed as revealed by the red-shifted fluorescence maximum at 350 nm in the *absence* of denaturant.

Kinetics of Unfolding of CCP(MI) and HRP in Denaturants. Exponential growth of the fluorescence intensity at

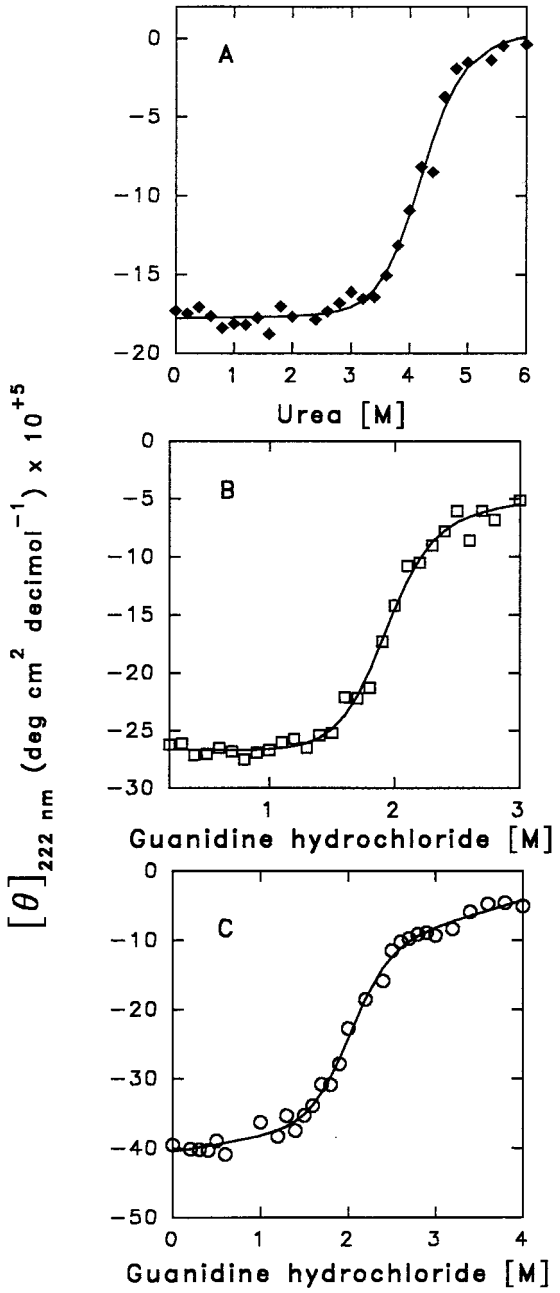

FIGURE 6: Molar ellipticity at 222 nm at pH 7.0 of (A) 4.7 μM CCP(MI) in urea, (B) 5.7 μM CCP(MI) in GdHCl, and (C) 5.9 μM HRP in GdHCl. The solid lines show the fit of the data by nonlinear least-squares analysis (Hughson & Baldwin, 1989; Betz & Pielak, 1992). The CD conditions are described in the text.

350 nm was observed on rapidly mixing the proteins with high concentrations of denaturants (data not shown). The intensity vs time data for CCP(MI) in 8 M urea and HRP in 6 M GdHCl at pH 7.0 were fit by single exponentials, and the half-lives ($t_{1/2}$) are listed in Table 2. CCP(MI) and HRP unfold in denaturant with $t_{1/2}$ values of 14.3 and 519 s, respectively. HRP treated with 3 mM DTT or 2 mM EDTA unfolds only slightly faster than untreated HRP, but denaturation in 4 M GdHCl of HRP treated with *both* DTT and EDTA occurs with $t_{1/2}$ = 0.42 s (Table 2). The large decrease in kinetic stability of HRP indicates that both types of stabilizing elements are removed on incubation with DTT *and* EDTA together.

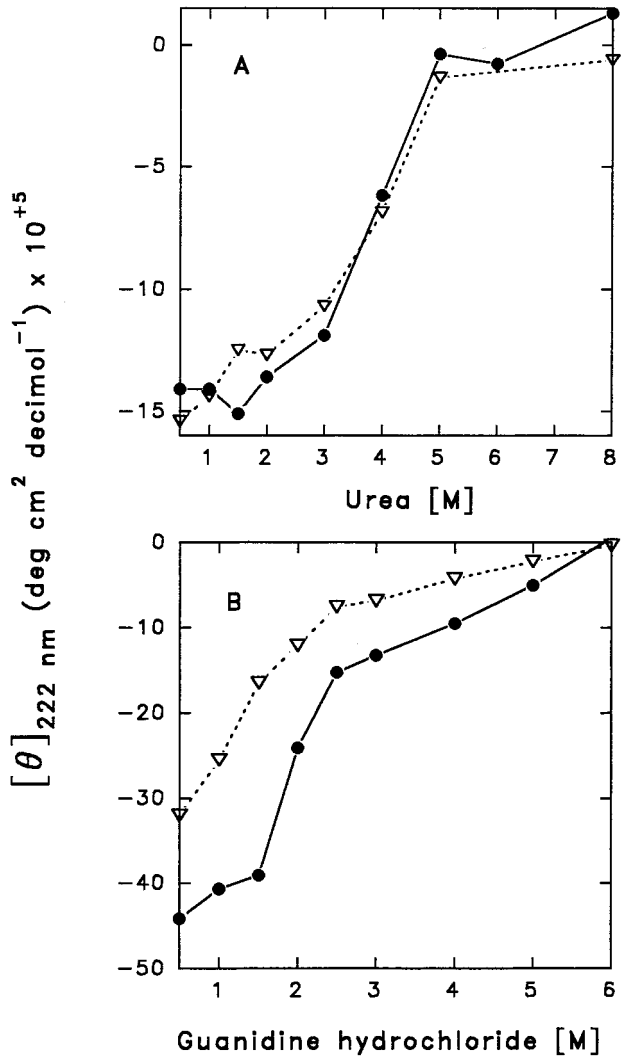

FIGURE 7: Molar ellipticity at 222 nm at pH 7.0 of (A) 5.2 μM CCP(MI) during unfolding (●) and refolding (▽) in urea and (B) 6.5 μM HRP during unfolding (●) and refolding (▽) in GdHCl. The CD conditions are described in the text.

Table 1: Thermodynamic Parameters for the Unfolding of CCP(MI) and HRP as Monitored by UV/CD

protein samples	$\Delta G_{d,aq}$ (kcal/mol)[a]	m (kcal mol^{-1} M^{-1})[a]	$[D]_{1/2}$[b] (M)
CCP(MI) in urea	6.2 ± 0.3 (3)[c]	1.5	4.2
CCP(MI) in GdHCl	6.4 ± 0.5 (2)[c]	3.4	1.9
HRP in GdHCl	4.0 ± 0.6 (2)[c]	2.0	2.0

[a] Calculated using the nonlinear least-squares analysis method of Hughson and Baldwin (1989) with $T = 298$ K. $\Delta G_{d,aq}$ represents the free energy in 0 M denaturant, and m is the slope of the linear dependence of ΔG_d on denaturant concentration (eq 6). The UV/CD data are from Figure 6. [b] Denaturant concentration at half-maximum ellipticity. [c] Number of separate determinations of $\Delta G_{d,aq}$.

DISCUSSION

Both steady-state fluorescence and circular dichroism are very useful techniques for studying the structure and dynamics of proteins (Beechem & Brand, 1985; Pace, 1986). The intrinsic fluorescence of proteins from residues such as Trp, Tyr, and Phe (Creighton, 1993) is an excellent built-in reporter. For example, the microenvironment surrounding Trp residues can be probed since these exhibit emission maxima that red-shift from ~320 to 350 nm as their

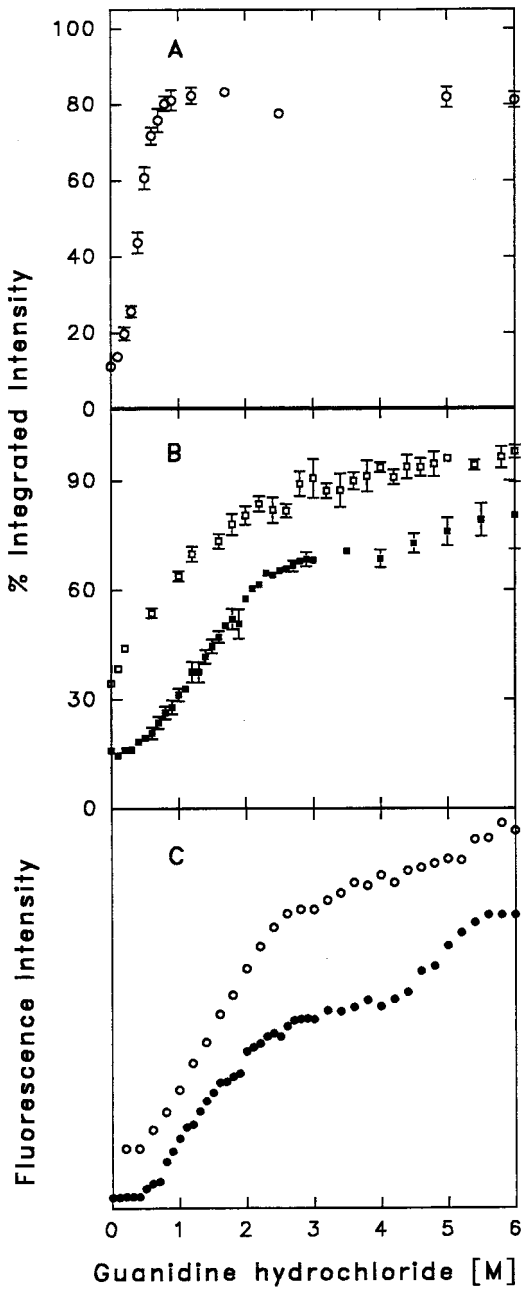

FIGURE 8: (A) Relative integrated fluorescence intensities (300−450 nm) vs GdHCl concentration at pH 7.0 of 2 μM EDTA-treated HRP. HRP (10 μM) was incubated for 18 h with 2 mM EDTA prior to dilution in GdHCl. Intensities are plotted relative to 2 μM NATA/10 μM NAYA treated with 2 mM EDTA, and the data points represent the average of two measurements. Excitation 280 nm; slits 5 nm; scan rate 102 nm/min. (B) Relative integrated fluorescence intensities (300−450 nm) vs GdHCl concentration at pH 7.0 of 2 μM HRP treated with 3 mM DTT (■) and 30 mM DTT (□). HRP (10 μM) was incubated for 18 h with DTT prior to dilution in GdHCl. Intensities are plotted relative to 2 μM NATA/10 μM NAYA treated with 3 mM DTT and 30 mM DTT, and the data points represent the average of two measurements. Excitation 280 nm; slits 5 nm; scan rate 102 nm/min. (C) Fluorescence intensity at 350 nm of untreated HRP (●) and 3 mM DTT-treated HRP (○). Excitation 295 nm; slits 5 nm; scan rate 402 nm/min. The fluorescence intensity curves of the two samples have been offset for clarity.

environment changes from nonpolar to polar (Burnstein et al., 1973). A fluorescence red-shift also occurs when Trps buried in a protein interior become solvent exposed as a result of denaturation. Unfolding of heme proteins generally results

Table 2: Half-Lives ($t_{1/2}$) for CCP(MI) and HRP Unfolding in Denaturants

protein samples	$t_{1/2}$ (s)[a]	n[b]
CCP(MI)[c]	14.3 ± 3.4	9
HRP[d]	519 ± 36	4
HRP + DTT[d,e]	450 ± 23	3
HRP + EDTA[d,e]	395 ± 37	4
HRP + DTT + EDTA[f]	0.420 ± 0.006	2

[a] Half-lives were obtained by fitting the fluorescence intensities at 350 nm vs time by first-order kinetics. [b] Number of observations. [c] 1 μM protein was rapidly mixed with 8 M urea at pH 7.0. [d] 2 μM protein was rapidly mixed with 6 M GdHCl at pH 7.0. [e] HRP was incubated for 18 h with 3 mM DTT or 2 mM EDTA prior to unfolding. [f] 5 μM HRP was rapidly mixed with 4 M GdHCl at pH 7.0 after an 18 h incubation with 3 mM DTT *and* 2 mM EDTA.

in a dramatic increase in steady-state protein fluorescence due to relief of heme quenching in the denatured state (Ugarova et al., 1981; Pappa & Cass, 1993; Fox et al., 1994; Moosavi-Movahedi & Nazari, 1995). In addition to fluorescence and CD, heme absorption is yet another useful conformational probe (Irace et al., 1986) for the study of heme proteins.

Denaturation of CCP(MI). CCP(MI), like the yeast form of the enzyme, contains seven Trps (Takio & Yonetani, 1980) which dominate the steady-state fluorescence of the protein (Fox et al., 1994). A low quantum yield due to efficient energy transfer to the heme is seen in the native protein (Figure 1A); however, the fluorescence exhibits a shift to longer wavelengths and increases in intensity when CCP(MI) is denatured in urea. The fluorescence emission of native CCP(MI) is independent of the excitation wavelength, and the protein exhibits a spectrum in 8 M urea (pH 7.0) similar to the Trp standard, NATA (Figure 1A and 1C), revealing that there is no fluorescence contribution from the 14 Tyr or 18 Phe residues (Takio & Yonetani, 1980), which as free amino acids in solution also have fluorescent properties (Creighton, 1993).

Denaturation of CCP(MI) is observed on incubation with increasing concentrations of both urea and GdHCl. The unfolding of CCP(MI) as examined by intrinsic fluorescence is not a simple two-state (N ⇌ U) process since stable thermodynamic intermediates are observed at 3−4 M urea and 1−2 M GdHCl (Figure 2A,B). Thermodynamically-stable unfolding intermediates have been observed with apo- and holoMb (Irace et al., 1986; Hughson & Baldwin, 1989), the α-subunit of tryptophan synthase (Matthews & Crisanti, 1981), α-lactalbumins (Murphy & Freire, 1992; Hayne & Freire, 1993), and porphyrin cytochrome *c* (Hu & English, unpublished results). Since Trp fluorescence in heme proteins is indirectly a measure of the Trp → heme energy transfer, formation of the unfolding intermediates in CCP(MI) most likely involves localized changes around the heme cavity that alter the energy-transfer efficiency. In support of this speculation, the heme CD absorption vs urea profile of CCP(MI) is also biphasic (Figure 4D), and the Soret absorption spectra recorded in 3.8 M urea and 1.3 M GdHCl suggest that the heme undergoes a transition from five-coordinate high-spin to six-coordinate low-spin prior to loss of secondary structure (Figure 4A,B) (Vitello et al., 1992).

Loss of CCP(MI) secondary structure appears to be a cooperative two-state process in both urea and GdHCl as monitored by backbone CD absorbance (Figure 6A,B). A comparison of the fluorescence and backbone CD curves (Figure 2A,B vs 6A,B) indicates that the fluorescence-sensitive intermediates are formed before the UV/CD-monitored loss of secondary structure occurs. In fact, the loss in secondary structure essentially coincides with the major fluorescence-detected I ⇌ U transition in CCP(MI) in both urea and GdHCl (Figure 2A,B). Furthermore, the Soret absorption spectra of CCP(MI) (Figure 4) reveal that heme loss from the polypeptide occurs mainly during the I ⇌ U transition, and the resultant heme spectra at high denaturant concentrations resemble those of free hemin shown in Figure 4C.

Calorimetry studies (Kresheck & Erman, 1988) have shown two midpoint transition temperatures (T_m) centered at 44 and 63 °C in the thermal denaturation of yeast CCP at pH 7.0. The first transition is accompanied by a temperature-induced shift in the Soret maximum from 408 to 414 nm, which was attributed to binding of a distal residue (most likely the distal His52) to the heme (Gross & Erman, 1985). Loss of secondary structure does not accompany the 44 °C transition, since the FTIR-monitored thermal denaturation of CCP(MI) revealed a single transition in the amide I′ region between 55 and 60 °C (Holzbaur et al., 1996), indicating loss of secondary structure over this narrow temperature range. However, the temperature dependence of the FTIR ν(CO) bands of the CO adduct of CCP(MI) revealed that the protein undergoes a conformational transition below 45 °C, which affects the heme pocket *prior* to loss of secondary structure (Holzbaur et al., 1996). Additionally, H ⇌ D exchange vs temperature, as monitored in the amide II region of the FTIR spectra of CCP(MI), indicated formation of an intermediate with partially collapsed tertiary structure and intact secondary structure (Holzbaur et al., 1996; van Stokkum et al., 1995). A similar mechanism could account for the N ⇌ I transition in the denaturant-induced unfolding of CCP(MI), leading to coordination of a sixth ligand to the heme (Figure 4A,B). It is of interest that a single endotherm was observed for heme-free apoCCP (Kresheck & Erman, 1988) with a T_m ∼60 °C, which corresponds to the higher T_m associated with secondary structure loss in holoCCP.

Denaturation of HRP. Isoenzyme C of HRP has a single Trp residue (Trp117; Welinder, 1979) which contributes to the fluorescence of the protein (Pappa & Cass, 1993). Denaturation of HRP also results in red-shifting of the fluorescence maximum as well as an increase in fluorescence intensity. Previous time-resolved fluorescence studies have shown that pH-induced conformational changes in HRP result in an increase in the fluorescence lifetime observed on the picosecond time scale (Das & Mazumdar, 1995). Unlike CCP(MI), excitation wavelength-dependent fluorescence is observed in HRP. There is a definite contribution to the intrinsic fluorescence of HRP from its five Tyr residues when 280-nm excitation is used (Das & Mazumdar, 1995), and the fluorescence spectra of HRP in >2 M GdHCl resemble that of a mixture of Trp and Tyr standards (Figure 1B,C).

It has been previously reported that HRP retains some activity and 50% secondary structure following incubation in 8 M urea (Pappa & Cass, 1993). Our observations also show that HRP exhibits <50% relative fluorescence in 8 M urea at pH 7.0. Increased interaction of GdHCl with the peptide groups of HRP was noted in a previous study on

urea and GdHCl denaturation of HRP (Moosavi-Movahedi & Nazari, 1995). Given the relatively weak effects of urea on HRP conformation, our present study focuses on GdHCl denaturation only.

Denaturation of HRP results in an intermediate (U′) with ~70% relative fluorescence between ~3 and 4 M GdHCl (Figure 2C). The single Trp (Trp117) in HRP is located in an extended chain between helix D and D′, on the basis of a comparison with the X-ray structure of PNP (Schuller et al., 1996; T. L. Poulos, personal communication). A *local* relaxation of this chain rather than a gross protein conformation change would account for the ~5% increase in relative fluorescence on 280-nm excitation that accompanies the U′ ⇌ U transition above 4 M GdHCl. Trp117 is preferentially excited at 295 nm (Das & Mazumdar, 1995), and no contribution to protein fluorescence at 350 nm is observed from Tyr on 295-nm excitation (Creighton, 1993). Hence, movement of the Trp117-containing extended chain in HRP during the U′ ⇌ U transition is supported by the dramatic increase in fluorescence above 4 M GdHCl on 295-nm excitation compared to that observed on 280-nm excitation (Figure 2C,D).

The GdHCl-induced changes in the UV/CD spectra of HRP (Figure 6C) support a two-state (N ⇌ U′) backbone unfolding process centered at 2.0 M GdHCl. The fluorescence-monitored U′ ⇌ U is a UV/CD-silent transition presumably since neither U′ nor U possesses secondary structure. The Soret absorption of HRP shows a large decrease between 1 and 3 M GdHCl (Figure 5), the denaturant concentrations that bracket the fluorescence- and UV/CD-monitored N ⇌ U′ transition (Figures 2C and 6C). Unlike CCP(MI), there is no red-shift in the Soret maximum of HRP in 1 M GdHCl; rather, a sharp crossover to solvent-exposed heme absorption is seen in denatured HRP at ≥2 M GdHCl (Figure 5A), and the heme CD spectra are also very similar to those of free heme at ≥2 M GdHCl (Figure 5B). Taken together, these observations indicate that heme loss in HRP is coincident with secondary structure loss during the N ⇌ U′ transition, and it is *not* preceded by formation of a heme cavity intermediate at low GdHCl concentrations as in CCP(MI) (Figure 4).

A recent FTIR investigation showed that HRP is thermally more stable than CCP(MI) since it loses its secondary structure at 90 °C, while that of CCP(MI) is lost at 55−60 °C (Holzbaur et al., 1996). A single T_m (~79 °C) was found for HRP using differential scanning calorimetry (Huddleston et al., 1995) suggesting, along with the FTIR studies of Holzbaur et al. (1996), that thermal denaturation of HRP is a two-state process. The FTIR spectra in the ν(CO) region also indicated that denaturation of the heme cavity coincides with the global thermal denaturation of HRP−CO (Holzbaur et al., 1996). Thus, the FTIR data and the denaturation data presented here provide strong evidence for a more stable heme pocket in HRP compared to CCP(MI).

Denaturation of EDTA- and DTT-Treated HRP. Enhanced conformational stability in native HRP is conferred by the presence of the bound Ca^{2+} ions and the four disulfide bridges (Haschke & Friedhoff, 1978; Smith et al., 1990; Pappa & Cass, 1993). Incubation with EDTA and DTT, which presumably chelates the bound ions (Smith et al., 1990; Pahari et al., 1995) and reduces the disulfide bonds (Creighton, 1990; Smith et al., 1990), respectively, results in a dramatic decrease in the kinetic stability of HRP as judged by the half-life of unfolding of the treated vs untreated protein in 4 M GdHCl ($t_{1/2}$ 0.4 vs 519 s). The X-ray structure of PNP (Figure 9) shows that a disulfide bridge (Cys44−Cys49) forms a loop encompassing several of the distal Ca^{2+} ligand residues (Schuller et al., 1996), and this same disulfide bridge is also seen in the X-ray structure of HRP (T. L. Poulos, personal communication). The half-life of unfolding of 2 mM EDTA-treated HRP is 26% lower than that of untreated HRP (Table 2). However, the significantly increased sensitivity of EDTA-treated HRP to denaturant ($[GdHCl]_{1/2}$ ~ 0.45 M; Figure 8A) suggests that thermodynamic stability is reduced more than kinetic stability on Ca^{2+} removal. Furthermore, the work of Pappa and Cass (1993) also demonstrated that apoHRP is more resistant to denaturation in the presence of Ca^{2+}, reinforcing a structural role for this cation in stabilizing the native conformation (Smith et al., 1990; Pahari et al., 1995). Of the two Ca^{2+} ions (Haschke & Friedhoff, 1978), one appears to be more important for maintaining the structure and function of HRP (Ogawa et al., 1979; Morishima et al., 1986; Shiro et al., 1986).

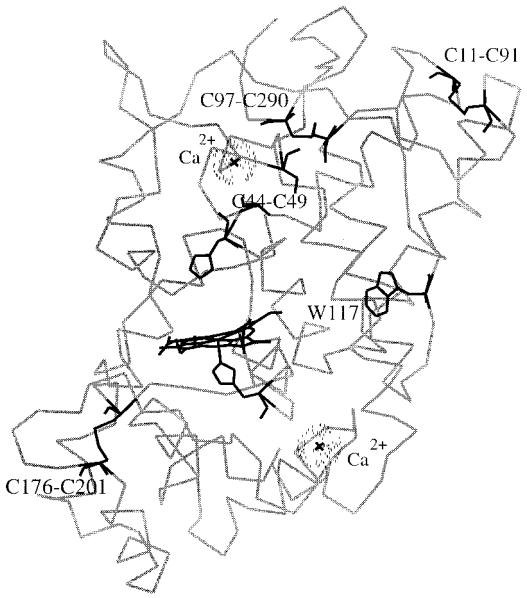

FIGURE 9: C_α backbone of PNP generated from the X-ray coordinates (Schuller et al., 1996). The heme, distal His42, proximal His169, Trp117, four disulfide bridges, and van der Waals radii of the two Ca^{2+} ions are shown in bold.

Calcium also seems to play an important role in PNP (Rodríguez Marañón et al., 1993), LIP (Doyle & Smith, 1996), and CIP (Tams & Welinder, 1996). While CCP does not bind cations, a proximal cation binding site has been engineered into the protein and was found to decrease the stability of the Trp191 radical in CCP compound I (Bonagura et al., 1996), which is formed on donation of two electrons to H_2O_2. In most peroxidases the two oxidizing equivalents of H_2O_2 are stored at the heme in the form of oxyferryl iron (Fe^{IV}═O) and a porphyrin π-cation radical (Dawson, 1988). CCP is the first known peroxidase to use a stable amino acid radical instead of a porphyrin π-cation radical in compound I, and the redox-active residue has been identified as Trp191 which lies within 5 Å of the heme (Sivaraja et al., 1989). Electrostatic calculations have shown that the proximal pocket in CCP is uniquely suited to stabilize the Trp191

radical (Miller et al., 1994); thus, although a proximal cation might increase the conformational stability of CCP, it would be counterproductive with respect to stabilization of protein-based radicals. APX, which contains a proximal cation (probably K^+) binding site and has Trp179 in a position analogous to Trp191 in CCP, does not form an amino acid radical during normal turnover (Patterson et al., 1995). Class II and III peroxidases (Welinder, 1992), which include HRP, PNP, CIP, and LIP, all contain both distal and proximal Ca^{2+} ions (Figure 9) for enhanced structural stability, but these peroxidases possess few oxidizable residues (English & Tsaprailis, 1995), suggesting that formation of protein-based radicals may not be important in these enzymes. It would be of interest to compare the thermodynamic and kinetic stabilities of APX and CCP(MI) (class I peroxidases) since, except for a proximal cation, APX does not possess other stabilizing elements (Patterson et al., 1995).

HRP treated with 3 and 30 mM DTT has intermediate GdHCl sensitivity ($[GdHCl]_{1/2} = 1.3$ and 0.9 M, respectively) compared to untreated HRP ($[GdHCl]_{1/2} = 2.0$ M) and EDTA-treated HRP ($[GdHCl]_{1/2} = 0.45$ M). This suggests that the reduced disulfide bridges contribute less than the bound Ca^{2+} ions to the thermodynamic stability of the native conformation of HRP. An inspection of the solvent accessibility of the four disulfide bridges in PNP (and presumably in HRP) shows that they are all solvent exposed (Figure 9). Cys11−Cys91 is the most solvent accessible followed by Cys97−Cys290, while Cys44−Cys49, which forms a loop encompassing several of the distal Ca^{2+} ligand residues in HRP, is the closest disulfide bridge to Trp117 at a distance of ∼11.4 Å (T. L. Poulos, personal communication). Pace and co-workers found that of the two disulfides in RNase T_1, the most solvent accessible is reduced first in the presence of 100 mM DTT (Pace et al., 1988). Hence, we speculate that Cys11−Cys91 is reduced first in folded HRP on incubation with 3 mM DTT, but since 30 mM DTT-treated HRP has ∼20% higher fluorescence than 3 mM DTT-treated HRP (Figures 2C and 8B), further disulfide reduction by the 10-fold extra free thiol must take place. Also, the fluorescence vs [GdHCl] profiles on excitation at 280 and 295 nm of DTT-treated HRP are similar in shape (Figure 8B,C), revealing that the U′ ⇌ U transition in the absence of DTT is due to conformational change around one or more disulfides.

Heme Capture and Thermodynamic Parameters. Although the UV/CD unfolding curves (Figure 6) suggest a simple N ⇌ U transition in both CCP(MI) and HRP, heme capture by the denatured peroxidases on refolding is remarkably different. The refolding data for CCP(MI) (Figures 3A,B and 7A) reveal that heme capture occurs at high denaturant concentrations, indicating that a non-native form of CCP(MI) recognizes heme. While heme incorporation in CCP(MI) coincides with refolding of the polypeptide, heme capture by HRP occurs *after* polypeptide refolding. This is supported by the observation that the secondary structure of HRP must be essentially reformed before heme capture occurs (Figures 3C and 7B) and by the fact that the heme CD spectra in 6−1 M GdHCl (not shown) resemble those of denatured HRP at ≥2 M GdHCl (Figure 5B). The Soret absorption measurements (not shown) confirm that heme capture by the polypeptide does occur below 1 M GdHCl and gives rise to the spectrum of native HRP.

Recently, proton NMR spectroscopy on a sperm whale Mb mutant (Lecomte et al., 1996) revealed the existence of well-folded regions in the apoprotein that are remarkably similar to the corresponding regions in the native holoprotein. A compact subdomain made up of the A−B−G−H helix interface in sperm whale apoMb (Takano, 1977) is speculated to represent the region of the folding intermediate responsible for heme capture. Formation of this compact subdomain, however, is not heme dependent since addition of free heme to folded apoMb results in a reconstituted Mb which has secondary structure and properties identical to those of native Mb (Pappa & Cass, 1993). In HRP, in addition to the requirement that the secondary structure be formed for heme capture *in vitro*, the distal His42 and proximal His170 also contribute to heme recognition since the His → Phe mutants, H42F and H170F, show altered kinetics of heme entrapment (Gazaryan et al., 1994).

The conformational stability of a protein that undergoes a reversible two-state N ⇌ U transition (eq 2) is given by its $\Delta G_{d,aq}$ (Pace, 1990a). The UV/CD-monitored unfolding of CCP(MI) and HRP (Figure 6) and refolding (Figure 7) curves suggest that secondary structure formation in the peroxidases follows a two-state reversible transition when allowance is made for the fraction of heme and polypeptide that undergoes precipitation. Thus, from the UV/CD data, $\Delta G_{d,aq}$ values of ∼6 and ∼4 kcal/mol are obtained for CCP(MI) and HRP, respectively (Table 1). These are at the low end of the range of values reported for globular proteins where the native state appears to be stabilized by 4−20 kcal/mol (Tanford, 1964; Rowe & Tanford, 1973; Pace & Vanderburg, 1979; Creighton, 1993). A $\Delta G_{d,aq}$ value of ∼6 kcal/mol was calculated for HRP at 25 °C and pH 6.4 in denaturants as studied by UV difference spectrophotometry (Moosavi-Movahedi & Nazari, 1995). The low $\Delta G_{d,aq}$ for HRP is surprising since the two bound Ca^{2+} ions and four disulfides are expected to yield a compact denatured state, which is inherently higher in energy than a fully extended polypeptide. Previous studies have shown that engineering artificial disulfide bonds into a protein enhances conformational stability by lowering the entropy of the unfolded state (Perry & Wetzel, 1984; Pantoliano et al., 1987; Pace et al., 1988; Matsumara et al., 1989; Gusev et al., 1991; Kanyaa et al., 1991). Nonetheless, the introduction of a single disulfide bond in yeast cytochrome *c* lowers $\Delta G_{d,aq}$ by ∼1 kcal/mol, despite the fact that the cross-link creates a compact denatured state (Betz & Pielak, 1992). It is of interest that DTT- and EDTA-treated HRP must possess a $\Delta G_{d,aq} < 0$ at room temperature since it exhibits high fluorescence intensity and an emission maximum at 350 nm in buffer only.

The *m* values calculated for the unfolding of CCP(MI) in urea and GdHCl are typical (∼1.5−2 kcal mol^{-1} M^{-1} in urea; ∼3−5 kcal mol^{-1} M^{-1} in GdHCl) of those seen in the denaturant-induced unfolding of heme proteins (Alonso & Dill, 1991). The 1.7-fold larger *m* value in GdHCl for CCP(MI) compared to HRP (Table 1) is an indication of increased cooperativity of unfolding in the former peroxidase. Cooperative unfolding is often observed with small (<20 kDa) single-domain proteins (Privalov, 1992), but it is also not uncommon to find multidomain proteins where the domains unfold cooperatively in a single transition (Griko et al., 1989; Pakula & Sauer, 1989). Multidomain proteins unfold with cooperativity in the presence of strong domain

interactions which cause mutual domain stabilization. The crystal structure of CCP shows that the protein is folded into two clearly defined domains (I and II) and that the heme occupies a crevice between them (Poulos et al., 1980). Hence, the highly cooperative unfolding of the secondary structure of CCP(MI) in GdHCl indicates strong interactions between domains I and II. The presence of disulfides in HRP might be responsible for the lower cooperativity of its secondary structure unfolding in GdHCl (Table 1) since, based on the sequence alignment of PNP, HRP, and CCP (Schuller et al., 1996), domains I and II of HRP are covalently bonded by the Cys97−Cys290 disulfide bridge. Furthermore, the work of Betz and Pielak (1992) has shown that a smaller *m* value is calculated for the cytochrome *c* Cys20−Cys102 cross-linked variant than for the non-crosslinked variant (2.7 vs 4.6 kcal mol^{-1} M^{-1}). Interestingly, the GdHCl concentration (∼2 M) at half-maximal backbone ellipticity ($[D]_{1/2}$) is almost the same for CCP(MI) and HRP. The $[D]_{1/2}$ was also reported to be approximately the same in non-cross-linked and cross-linked cytochrome *c* (Betz & Pielak, 1992).

The unfolding rates of CCP(MI) and HRP (Table 2) show that the native form of CCP(MI) unfolds significantly faster in high denaturant concentrations ($t_{1/2} \sim 14$ s) than HRP ($t_{1/2} \sim 519$ s), which reveals the higher kinetic stability of HRP. This is due to the presence of its stabilizing structural elements (two Ca^{2+} ions and four disulfide bridges), since removal of these elements gives rise to a protein which is both kinetically (Table 2) and thermodynamically highly unstable.

Conclusions. Despite the similar tertiary structures of CCP(MI) and HRP, their denaturation/renaturation and heme capture mechanisms in denaturants differ. Furthermore, the unfolding rates of the two peroxidases indicate that HRP is kinetically more stable than CCP(MI). The kinetic stability of HRP is associated with its bound Ca^{2+} ions and disulfides since their removal *greatly* destabilizes the protein. The kinetic stability of native HRP makes it an ideal protein for use in biotechnology (Ryan et al., 1994), while the greater conformational flexibility of CCP presumably facilitates radical generation, stabilization, and translocation within its polypeptide matrix (English & Tsaprailis, 1995). Also, such flexibility should facilitate heme capture by the apoCCP, which is the dominant form *in vivo* when yeast are grown under anaerobic conditions (Djavadi-Ohaniance et al., 1978).

ACKNOWLEDGMENT

We thank Dr. Mark Miller (UCSD) for providing the *E. coli* transformed with recombinant cytochrome *c* peroxidase used to isolate the CCP(MI) for this study. Professor Oswald Tee and Dr. Timothy Gadosy are thanked for their assistance with the stopped-flow experiments. Craig Fenwick is thanked for many helpful discussions and Yazhen Hu for her technical assistance. We also thank Professor Joanne Turnbull for critically reading the manuscript.

REFERENCES

Alonso, D. O. V, & Dill, K. A. (1991) *Biochemistry 30*, 5974.
Beechem, J. M., & Brand, L. (1985) *Annu. Rev. Biochem. 54*, 43.
Betz, S. F., & Pielak, G. J. (1992) *Biochemistry 31*, 12337.
Bonagura, C. A., Sundaramoorthy, M., Pappa, H. S., Patterson, W. R., & Poulos, T. L. (1996) *Biochemistry 35*, 6107.
Bosshard, R. H., Anni, H., & Yonetani, T. (1991) in *Peroxidases in Chemistry and Biology* (Everse, J., Everse, K. E., & Grisham, M. B., Eds.) Vol. II, pp 51−84, CRC Press, Boca Raton, FL.
Burnstein, E. A., Vedenkina, N. S., & Ivkova, M. N. (1973) *Photochem. Photobiol. 18*, 263.
Creighton, T. E. (1990) in *Protein Structure: A Practical Approach* (Creighton, T. E., Ed.) pp 155−167, IRL Press at Oxford University, Oxford, UK.
Creighton, T. E. (1993) in *Proteins: Structure and Molecular Properties*, Freeman, New York.
Das, T. K., & Mazumdar, S. (1995) *Eur. J. Biochem. 227*, 823.
Dawson, J. E. (1988) *Science 240*, 433.
Djavadi-Ohaniance, L., Rudin, Y., & Schatz, G. (1978) *J. Biol. Chem. 253*, 4402.
Doyle, W. A., & Smith, A. T. (1995) *Biochem. J. 315*, 15.
Dunford, H. B. (1991) in *Peroxidases in Chemistry and Biology* (Everse, J., Everse, K. E., & Grisham, M. B., Eds.) Vol. II, pp 1−24, CRC Press, Boca Raton, FL.
Edelhoch, H. (1967) *Biochemistry 6*, 1948.
English, A. M., & Tsaprailis, G. (1995) *Adv. Inorg. Chem. 43*, 79.
Finzel, B. C., Poulos, T. L., & Kraut, J. (1984) *J. Biol. Chem. 259*, 13027.
Fishel, L. A., Villafranca, J. E., Mauro, J. M., & Kraut, J. (1987) *Biochemistry 26*, 351.
Fox, T., Tsaprailis, G., & English, A. M. (1994) *Biochemistry 33*, 186.
Garavito, R. M., Picot, D., & Loll, P. J. (1994) *Curr. Opin. Struct. Biol. 4*, 529.
Garel, J.-R. (1992) in *Protein Folding* (Creighton, T. E., Ed.) pp 405−454, Freeman, New York.
Gazaryan, I. G., Doseeva, V. V., Galkin, A. G., & Tishkov, V. I. (1994) *FEBS Lett. 354*, 248.
Griko, Y. V., Venyaminov, S. Y., & Privalov, P. L. (1989) *FEBS Lett. 244*, 276.
Gross, T. M., & Erman, J. E. (1985) *Biochim. Biophys. Acta 830*, 140.
Gusev, N. B., Grabarek, Z., & Gergely, J. (1991) *J. Biol. Chem. 266*, 16622.
Haschke, R. H., & Friedhoff, J. M. (1978) *Biochem. Biophys. Res. Commun. 80*, 1039.
Hayne, D. T., & Freire, E. (1993) *Proteins: Struct., Funct., Genet. 16*, 115.
Holzbaur, I. E., English, A. M., & Ismail, A. A. (1996) *Biochemistry 35*, 5488.
Huddleston, S., Robertson, S., Dobson, C., Kwong, F. Y. P., & Charalmbous, B. M. (1995) *Biochem. Soc. Trans. 23*, 108S.
Hughson, F. M., & Baldwin, R. L. (1989) *Biochemistry 28*, 4415.
Irace, G., Bismuto, E., Savy, F., & Colonna, G. (1986) *Arch. Biochem. Biophys. 244*, 459.
Kahn, P. C. (1979) *Methods Enzymol. 61*, 339.
Kanaya, S., Katsuda, C., Kimura, S., Nakai, T., Kitakuni, E., Nakamura, H., Katayamagi, K., Morikawa, K., & Ikehara, M. (1991) *J. Biol. Chem. 266*, 6038.
Kresheck, G. C., & Erman, J. E. (1988) *Biochemistry 27*, 2490.
Kunishima, N., Fukuyama, K., Matsubara, H., Hatanakana, H., Shibano, Y., & Amalhi, T. (1994) *J. Mol. Biol. 235*, 331.
Lecomte, J. T. J., Kao, Y., & Cocco, M. J. (1996) *Proteins: Struct., Funct., Genet. 25*, 267.
Matsamura, M., Becktel, W. J., Levitt, M., & Matthews, B. W., (1989) *Proc. Natl. Acad. Sci. U.S.A. 86*, 6562.
Matthews, C. R., & Crisanti, M. M. (1981) *Biochemistry 20*, 784.
Miller, M. A., Shaw, A., & Kraut, J. (1994) *Nat. Struct. Biol. 1*, 524.
Moosavi-Movahedi, A. A., & Nazari, K. (1995) *Int. J. Biol. Macromol. 17*, 43.
Morishima, I., Kurono, M., & Shiro, Y. (1986) *J. Biol. Chem. 261*, 9391.
Murphy, K. P., & Freire, E. (1992) *Adv. Protein Chem. 41*, 313.
Ogawa, S., Shiro, Y., & Morishima, I. (1979) *Biochem. Biophys. Res. Commun. 90*, 674.
Pace, C. N. (1986) *Methods Enzymol. 131*, 266.
Pace, C. N. (1990) *Trends Biotechnol. 8*, 93.
Pace, C. N., & Vanderburg, K. E. (1979) *Biochemistry 18*, 288.

Pace, C. N., Grimsley, G. R., Thomson, J. A., & Barnett, B. J. (1988) *J. Biol. Chem. 263*, 11820.
Pace, C. N., Shirley, B. R., & Thomson, J. A. (1990) in *Protein Structure: A Practical Approach* (Creighton, T. E., Ed.) pp 311−330, IRL Press at Oxford University, Oxford, UK.
Pahari, D., Patel, A. B., & Behere, D. V. (1995) *J. Inorg. Biochem. 60*, 245.
Pakula, A. A., & Sauer, R. T. (1989) *Proteins: Struct., Funct., Genet. 5*, 202.
Pantoliano, M. W., Landner, R. C., Bryan, P. N., Rollence, M. L., Wood, J. F., & Poulos, T. L. (1987) *Biochemistry 26*, 2077.
Pappa, H. S., & Cass, A. E. G. (1993) *Eur. J. Biochem. 212*, 227.
Patterson, W. R., & Poulos, T. L. (1995) *Biochemistry 34*, 4331.
Patterson, W. R., Poulos, T. L., & Goodin, D. B. (1995) *Biochemistry 34*, 4342.
Perry, L. J., & Wetzel, R. (1984) *Science 226*, 555.
Petersen, J. F. W., Kadziola, A., & Larsen, S. (1994) *FEBS Lett. 339*, 291.
Poulos, T. L. (1993) *Curr. Opin. Biotechnol. 4*, 484.
Poulos, T. L., & Fenna, R. E. (1994) in *Metal Ions in Biological Systems: Metalloenzymes Involving Amino Acid-Residue and Related Radicals* (Siegel, H., & Sigel, A., Eds.) Vol. 30, pp 25−75, Marcel Dekker, Monticello, NY.
Poulos, T. L., Freer, S. T., Alden, R. A., Edwards, S. L., Skogland, U., Takio, K., Eriksson, B., Xuong, N. H., Yonetani, T., & Kraut, J. (1980) *J. Biol. Chem. 255*, 575.
Poulos, T. L., Edwards, S. L., Wariishi, H., & Gold, M. H. (1993) *J. Biol. Chem. 268*, 4429.
Privalov, P. L. (1992) in *Protein Folding* (Creighton, T. E., Ed.) pp 243−300, Freeman, New York.
Rainer, J., & Rainer, R. (1990) in *Protein Structure: A Practical Approach* (Creighton, T. E., Ed.) pp 191−223, IRL Press at Oxford University, Oxford, UK.
Rodríguez Marañón, M. J., Stillman, M. J., & van Huystee, R. B. (1993) *Biochem. Biophys. Res. Commun. 194*, 326.
Rowe, E. S., & Tanford, C. (1973) *Biochemistry 12*, 4822.
Ryan, O., Smyth, M. R., & Ó Fágáin, C. (1994) *Enzyme Microb. Technol. 16*, 501.
Schuller, D. J., Ban, N., van Huystee, R. B., McPherson, A., & Poulos, T. L. (1996) *Structure 4*, 311.
Shiro, Y., Nurono, M., & Morishima, I. (1986) *J. Biol. Chem. 261*, 9382.
Sievers, G. (1978) *Biochim. Biophys. Acta 536*, 212.
Sivaraja, M., Goodin, D. B., Smith, M., & Hoffman, B. M. (1989) *Science 245*, 738.
Smith, A. T., Santama, N., Dacey, S., Edwards, M., Bray, R. C., Thorneley, R. N. F., & Burke, J. F. (1990) *J. Biol. Chem. 265*, 13335.
Sundaramoorthy, M., Kishi, K., Gold, M. H., & Poulos, T. L. (1994) *J. Biol. Chem. 269*, 32759.
Takano, T. (1977) *J. Mol. Biol. 110*, 537.
Takio, K., & Yonetani, T. (1980) *Arch. Biochem. Biophys. 203*, 605.
Tams, J. W., & Welinder, K. G. (1996) *Biochemistry 35*, 7573.
Tanford, C. (1964) *J. Am. Chem. Soc. 86*, 2050.
Ugarova, N. N., Savitski, A. P., & Berezin, I. V. (1981) *Biochim. Biophys. Acta 662*, 210.
van Stokkum, I. H. M., Linsdell, H., Hadden, J. M., Haris, P. I., Chapman, D., & Bloemendal, M. (1995) *Biochemistry 34*, 10518.
Veitch, N. C., & Williams, R. J. P. (1990) *Eur. J. Biochem. 189*, 351.
Vitello, L. B., Erman, J. E., Miller, M. A., Mauro, J. M., & Kraut, J. (1992) *Biochemistry 31*, 11524.
Welinder, K. G. (1979) *Eur. J. Biochem. 96*, 483.
Welinder, K. G. (1992) *Curr. Opin. Struct. Biol. 2*, 388.
Willis, K. J., Szabo, A. G., Zuker, M., Ridgeway, J. M., & Alpert, B. (1990) *Biochemistry 29*, 5270.

BI971032A